Stress, September 2012; 15(5): 514–523

ISSN 1025-3890 print/ISSN 1607-8888 online
DOI: 10.3109/10253890.2011.643516

informa
healthcare

Wistar rats subjected to chronic restraint stress display increased hippocampal spine density paralleled by increased expression levels of synaptic scaffolding proteins

D. ORLOWSKI[1], B. ELFVING[2], H. K. MÜLLER[2], G. WEGENER[2], & C. R. BJARKAM[1,3]

[1]*Department of Biomedicine, Faculty of Health Sciences, Aarhus University, Aarhus C, Denmark,* [2]*Centre for Psychiatric Research, Aarhus University Hospital, Risskov, Denmark, and* [3]*Department of Neurosurgery, Aarhus University Hospital, Aarhus C, Denmark*

(*Received 2 March 2011; revised 9 September 2011; accepted 6 November 2011*)

Abstract
The aim of this study was to investigate whether the previously reported effect of chronic restraint stress (CRS) on hippocampal neuron morphology and spine density is paralleled by a similar change in the expression levels of synaptic scaffolding proteins. Adult male Wistar rats were subjected either to CRS (6 h/day) for 21 days or to control conditions. The resulting brains were divided and one hemisphere was impregnated with Golgi-Cox before coronal sectioning and autometallographic development. Neurons from CA1, CA3b, CA3c, and dentate gyrus (DG) area were reconstructed and subjected to Sholl analysis and spine density estimation. The contralateral hippocampus was used for quantitative real-time polymerase chain reaction and protein analysis of genes associated with spine density and morphology (the synaptic scaffolding proteins: Spinophilin, Homer1-3, and Shank1-3). In the CA3c area, CRS decreased the number of apical dendrites and their total length, whereas CA1 and DG spine density were significantly increased. Analysis of the contralateral hippocampal homogenate displayed an increased gene expression of Spinophilin, Homer1, Shank1, and Shank2 and increased protein expression of Spinophilin and Homer1 in the CRS animals. In conclusion, CRS influences hippocampal neuroplasticity by modulation of dendrite branching pattern and spine density paralleled by increased expression levels of synaptic scaffolding proteins.

Keywords: *Neuroplasticity, Sholl analysis, postsynaptic density proteins, Golgi-Cox impregnation, fractal analysis, real-time qPCR, Western blotting*

Introduction

Brain functionality and health depend on the ability of neural cells to alter their connectivity by morphological changes in branching pattern and synapse formation/reorganization (Bartesaghi et al. 2003; Cook and Wellman 2004; Shi et al. 2004; Alquicer et al. 2008; Campana et al. 2008). Recent animal studies have indicated that such changes may occur in depression-like stress conditions, which may lead to a decreased number of dendritic branches and fewer synapses in the hippocampus and prefrontal cortex (Woolley et al. 1990; Watanabe et al. 1992; McEwen 1999; Bartesaghi et al. 2003; Pham et al. 2003; Cook and Wellman 2004; Alquicer et al. 2008). The hippocampus is especially rich in glucocorticoid receptors and accordingly has been shown to be particularly affected by high cortisol levels generated by repeated stress, leading to remodeling of the CA3 dendritic tree, formation of CA1 dendritic spines, and suppression of the synaptic activity and altered neurogenesis (McLaughlin et al. 2007; McEwen 2008; Tata and Anderson 2010). In rats, such changes have been accompanied by a deficit in hippocampal functions, including learning and spatial memory (McLaughlin et al. 2007). Many experiments show that the type of stress is important, and that various stressors and stress length may lead to diverse effects in different organisms. Likewise, the consequences of

Correspondence: D. Orlowski, Department of Biomedicine, Wilhelm Meyers Allé 3, DK-8000, Aarhus C, Denmark. Tel: + 45 87167632. Fax: + 45 86198664. E-mail: dorl@ana.au.dk; dariusz.orlowski@gmail.com

stress depend on the animal sex and the content of the sex hormones in blood (Shors et al. 2004; Brusco et al. 2008; Koolhaas et al. 2011; Parihar et al. 2011). For example, 21 days of restraint stress induced dendritic atrophy in the CA3 hippocampal subregion in Sprague-Dawley rats, whereas 14 days of restraint stress did not cause any significant changes (Magarinos and McEwen 1995a; McLaughlin et al. 2007; Hageman et al. 2009).

The aim of the present study was to examine how the 21-day restraint stress paradigm influences spine formation and cell morphology in the hippocampus of Wistar rats. Furthermore, it was investigated whether such changes in dendrite morphology and spine density were paralleled by changes in the expression levels of the synaptic scaffolding proteins, Spinophilin, Homer, and Shank, as previous studies have provided evidence for a role of these proteins in the regulation of spine morphology and density (Feng et al. 2000; Sala et al. 2001; Sarrouilhe et al. 2006).

Materials and methods

Animals and experimental groups

Twenty-eight male Wistar rats (aged 9–10 weeks, weighing approximately 300 g, Taconic MB, Ry, Denmark) were used in this study in accordance with the guidelines issued by the Danish National Committee for Ethics in Animal Experimentation (authorization number: 2007/561-1378). The animals were housed in pairs (Cage 1291H Eurostandard Type III H, 425 × 266 × 185 mm, Techniplast, Buguggiate, Italy) at 20 ± 2°C in a 12-h light–dark cycle (lights on at 7.00 am) with free access to food and water. The animals were randomly assigned into two groups ($n = 14$ in each group): (1) rats subjected to 6 h daily restraint stress for 21 days (chronic restraint stress, CRS) and (2) control rats (CON).

Restraint stress paradigm

During the stress period, CON remained in their home cages with daily handling. In a separate room, the stress group was subjected to a 6-h daily restraint stress schedule (9.00 am to 3.00 pm) for 21 days in transparent acrylic restrainers secured at the head and tail (Watanabe et al. 1992; Magarinos and McEwen 1995b; Hageman et al. 2008), with an intensive light source above (1000 lux) (Vestergaard-Poulsen et al. 2011). To protect the CRS animals from overheating, the acrylic restrainers contained drilled holes (1 per 3 cm^2).

Tissue collection

After completion of restraint stress procedures, the animals were killed by decapitation the following day (18 h after last CRS procedure ended) and the brains removed immediately after. The fresh brains were divided into two halves mid-sagitally, one half (randomized) was subjected to histochemistry, whereas the other half was subjected to molecular biological analysis.

Histochemistry

The brain halves for histochemistry were initially immersed in 100 ml of phosphate buffered 4% paraformaldehyde (pH 7.4) for 3 weeks. The brains were then impregnated for 21 days in a Golgi-Cox solution (Orlowski and Bjarkam 2009), followed by immersion in 30% sucrose for 5 days, before vibratome sectioning into 100 μm coronal sections. The free flowing sections were transferred into ammonium hydroxide (28% solution diluted 1:1 with distilled water immediately before use) for 30 min (Gibb and Kolb 1998) and subjected to autometallographic development to enhance the staining pattern as described by Orlowski and Bjarkam (2009).

Image analysis for spine density and cell morphology

Dendritic spines were counted blind to the experimental condition. Measurements were obtained from the dorsal hippocampus in the following areas: CA1, CA3b, CA3c, and dentate gyrus (DG) (Figure 1A). Secondary or tertiary dendritic branches from the apical part (stratum radiatum) and the basal part (stratum oriens) of CA1 and CA3, and dendritic branches located in the outer half of the DG molecular layer were analyzed (Figure 1A). Dendritic fragments used for analysis met the following criteria: (1) good staining and impregnation without breaks (Figure 1B), (2) location about 150 μm (apical part) or about 40 μm (basal part) from soma or about 100 μm from soma for DG granular cells (Figure 1A), (3) branch fragments must be in the same focus plane and have a length about 30 μm (20–50 μm) (Figure 1B4–6). From each hippocampal subregion, at least eight fragments per brain were analyzed (more than 100 analyzed fragments per region per group). Spines were counted in the ImageJ program (Rasband, W.S., ImageJ, US National Institutes of Health, Bethesda, Maryland, USA, http://rsb.info.nih.gov/ij/, 1997–2005) on photographs taken with a Leica DFC 480 camera mounted on a Leica DM5000B microscope using 40 × objectives. With this magnification, spines were clearly visible (Figure 1B4–6), and the counting was done using an additional 3 × digital zoom. All protrusions from the dendrites were treated as "spines", and only spines distinct from the dendritic branch were counted. The number of spines obtained is likely to represent underestimates of the actual spine density because no attempt was made to correct for spines hidden beneath or above the dendritic segment (Gonzalez and Kolb 2003). For morphological

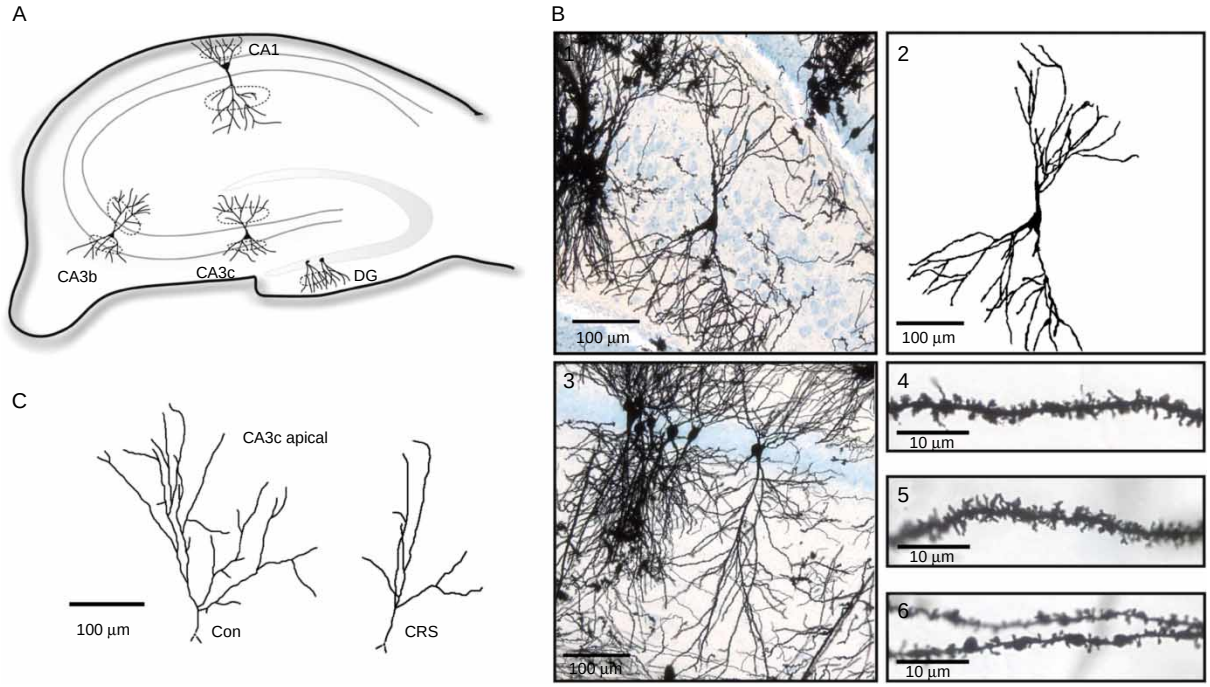

Figure 1. (A) Schematic diagram of the rat hippocampus; cell morphology and spine density were analyzed in marked areas. (B) Examples of neurons and dendritic fragments from Golgi-Cox stained rat hippocampus (CRS group): 1, microphotograph of CA3c pyramidal cell; 2, reconstruction of the cell seen in 1; 3, microphotograph of CA1 pyramidal cell; 4 and 5, fragments of dendrites from CA1 with visible spines; 6, fragment of a DG granular cell dendrite. (C) Illustration of CA3c pyramidal cell apical branches from the control and the CRS group, respectively.

analysis, neurons from CA1, CA3b, CA3c, and DG were selected for reconstruction if they fulfilled the following criteria: (1) consistent impregnation through the whole cell, (2) absence of obviously cut branches, (3) relative isolation from neighboring cells, and (4) cell bodies in the middle third of the tissue section in order to avoid analysis of cells with dendritic branches extending outside the section (Magarinos and McEwen 1995a). The selected neurons were observed using a Leica DM5000B bright field microscope with a 20 × objective and photographed with a Leica DFC 480 digital camera on different focus planes to ensure that the entire 3D structure of the dendrites was on the photographs, although reconstruction was done in 2D. Neurons were reconstructed in the freeware Neuromantic program (http://www.rdg.ac.uk/neuromantic/) (Figure 1B2) and analyzed with the ImageJ program.

The neuronal branching pattern was quantified using the Sholl analysis (Sholl 1953) and analysis the fractal dimension (FD) of the neuronal skeleton was calculated using ImageJ plugins (http://www-biology.ucsd.edu/labs/ghosh/software/ShollAnalysis_.class for Sholl analysis and http://rsbweb.nih.gov/ij/plugins/fraclac/fraclac.html for fractal analysis using box-counting method). Moreover, the number of terminal branches and the total length of the dendritic tree were calculated. As relatively few CA3c cells fulfilled our reconstruction criteria for cells (due to overlapping or incomplete basal part), only the apical part of these cells was reconstructed and analyzed (Figure 1C).

Measurements of mRNA levels with quantitative real-time polymerase chain reaction

The hippocampus from the other brain half was dissected and frozen on dry ice powder. It was stored at − 80°C until use. The hippocampus was homogenized in lysis buffer (Applied Biosystems, Carlsbad, CA, USA) with mixer-mill (Retsch, Haan, Germany) 2 × 1 min (30 Hz) for subsequent RNA characterization, cDNA synthesis, and quantitative real-time polymerase chain reaction (real-time qPCR) as previously described (Elfving et al. 2008). The Paris™ RNA and protein isolation kit (Ambion, Austin, TX, USA) were used to isolate hippocampal RNA and protein. The fraction to be used for protein quantification was processed as specified under "immunoblotting", and the fraction to be used for RNA isolation was immediately mixed with an equal volume of 2 × lysis/binding solution at room temperature (RT). Subsequently, one sample volume of 100% ethanol was added to the tube and mixed. The sample mixture was applied to a filter cartridge assembled in a collection tube and centrifuged for 1 min at 13,000*g*. The sample was washed with 700 µl Wash Solution 1, and twice with 500 µl Wash Solution 2/3. Each washing step was followed by centrifugation (13,000*g*, 1 min). The RNA was eluted with two

sequential aliquots (25 μl) of hot Elution Solution (~95°C) followed by centrifugation (13,000*g*, 30 s). Aliquots of the RNA solution were taken for both RNA quantification and qualification. The integrity of the RNA and the RNA concentration was determined with RNA StdSens microfluidic chips using the Experion Automated Electrophoresis System (Biorad, Hercules, CA, USA). The RNA purity and the RNA concentration were determined by spectrophotometer (Nanodrop 1000, Thermo Scientific, Billerica, MA, USA). Data on the quality and purity of the extracted RNA were evaluated with student's *t*-test. Afterwards, RNA was reversely transcribed using random primers and superscript III Reverse Transcriptase (Invitrogen, Carlsbad, CA, USA) following the manufacturer's instructions and with an RNA concentration per reaction of 28 ng/μl. The cDNA samples were diluted 1:30 with diethylpyrocarbonate (DEPC) water before used as a qPCR template.

Real-time qPCR

Real-time qPCR reactions were carried out in 96-well PCR-plates using the Mx3000P (Stratagene, La Jolla, CA, USA) and SYBR Green. Each SYBR Green reaction (10 μl total volume) contained 1 × SYBR Green master mix (Biorad), 0.5 μM primer pairs, and 3 μl of diluted cDNA. The gene expression of Spinophilin, Homer1-3, Shank1-3, and eight different reference genes (18s subunit ribosomal RNA (18s rRNA), beta-actin (ActB), cyclophilin A (CycA), glyceraldehyde-3-phosphate dehydrogenase (Gapd), hydroxy-methylbilane synthase (Hmbs), hypoxanthine guanine phosphoribosyl transferase 1 (Hprt1), ribosomal protein L13A (Rpl13A), tyrosine 3-monooxygenase/tryptophan 5-monooxygenase activation protein, zeta (Ywhaz)) was investigated. The reference genes were selected as described previously (Bonefeld et al. 2008). The primers were designed and tested as described by Elfving et al. (2008).

The following forward and reverse primers were used: Spinophilin forward: TCCTGTGGAGTTGGAGAAGG, reverse: TGCCTTTGGTGTTCCTAAGC (239 bp); Homer1 forward: CACCCGATGTGACACAGAAC, reverse: TGTTGCTTCCACTGCTTCAC (220 bp); Homer2 forward: CTGCCAGGTTAGCCAGAGAC, reverse: TCTTCACATTGGCAGCACTC (219 bp); Homer3 forward: GGTCAAAGAAGCTGCCAGAC, reverse: TGCGGAACAGCTTCTCTTCT (143 bp); Shank1 forward: CACTCTCAGCACCTGGAACA, reverse: GAAGGGTGTCTGTCCGTTGT (177 bp); Shank2 forward: CCTCCAGGACTGCAGAGAAC, reverse: ATTTCTGCCTTCGCATCGTA (204 bp); Shank3 forward: CTGTGTGGAGGAAGTGCAGA, reverse: GAACAAAGCCAAAACCCTCA (188 bp); 18s rRNA forward: ACGGACCAGAGCGAAAGCAT, reverse: TGTCAATCCTGTCCGTGTCC (310 bp); ActB forward: TGTCACCAACTGGGACGATA, reverse: GGGGTGTTGAAGGTCTCAAA (165 bp); CycA forward: AGCACTGGGGAGAAAGATT, reverse: AGCCACTCAGTCTTGGCAGT (248 bp); Gapd forward: TCACCACCATGGAGAAGGC, reverse: GCTAAGCAGTTGGTGGTGCA (168 bp); Hmbs forward: TCCTGGCTTTACCATTGGAG, reverse: TGAATTCCAGGTGAGGGAAC (176 bp); Hprt1 forward: GCAGACTTTGCTTTCCTTGG, reverse: CGAGAGGTCC TTTTCACCAG (81 bp); Rpl13A forward: ACAAGAAAAAGCGGATGGTG, reverse: TTCCGGTAATGGATCTTTGC (167 bp); Ywhaz forward: TTGAGCAGAAGACGGAAGGT; reverse: GAAGCATTGGGGATCAAGAA (136 bp). The primers were obtained from DNA Technology A/S (Risskov, Denmark).

For data normalization, we first measured mRNA levels for the reference genes. Stability comparison of the expression of the reference genes was conducted with the Normfinder software (http://www.mdl.dk) (Andersen et al. 2004). Ywhaz and Actb were determined to be the best combination in the hippocampus, and therefore values for each individual were normalized with the geometric mean of these reference genes.

Immunoblotting

Aliquots of total homogenate from individual animals, obtained using the Paris™ RNA and protein isolation kit (Ambion), were diluted in lysis buffer [50 mM Tris–HCl, pH 7.4, 150 mM NaCl, 1% Triton X-100, 0.1% sodium dodecyl sulfate (SDS), 2 mM EDTA and 1 × proteinase inhibitor cocktail (Roche, Mannheim, Germany)] to a final protein concentration of 2 μg/μl. After 30 min on ice, samples were clarified by centrifugation for 2 min at 12,000*g*. Aliquots of supernatants were mixed with SDS-sample buffer (125 mM Tris–HCl, pH 6.8, 20% glycerol, 4% SDS, 0.02% bromophenol blue, and 125 mM dithiothreitol), incubated at 55°C for 15 min and analyzed by SDS–polyacrylamide gel electrophoresis using 10% precast NuPAGE gels (Invitrogen) with a 3-(N-morpholino)-propanesulfonic acid (MOPS) buffer system. Proteins were transferred onto nitrocellulose membranes using the iBlot dry blotting system (Invitrogen). The membranes were blocked with 5% dry milk in Tris-Buffered Saline and Tween 20 (TBS-T) (50 mM Tris–HCl, pH 8.0, 150 mM NaCl, and 0.5% Tween 20) for 1 h at RT and probed with the primary antibodies: goat polyclonal anti-Spinophilin (1:500), mouse monoclonal anti-Homer1 (1:400) (Santa Cruz Biotechnology, Santa Cruz, CA, USA), and mouse monoclonal anti-glyceraldehyde 3-phosphate dehydrogenase (GAPDH) (1:1000) (Abcam, Cambridge, UK), overnight at 4°C followed by incubation with the appropriate horseradish peroxidase (HRP)-conjugated secondary antibody for 2 h at RT: rabbit polyclonal anti-goat antibody (1:10,000) (Santa Cruz Biotechnology) or goat polyclonal anti-mouse antibody (1:2000) (Pierce, Rockford,

IL, USA). Immunoreactive bands were visualized using ECL Advance Western Blotting Detection Reagent (GE Healthcare, Buckinghamshire, UK). The chemiluminescent signals were captured on a KODAK Image Station 440 and relative intensities were quantified by the KODAK 1D3.6 Image Analysis Software.

Statistical analysis

For statistical analysis of the group differences, a *t*-test with significance level $p < 0.05$ was used with one factor (CRS/no CRS) and two outcome groups. The Sholl analysis-based comparison of the branching pattern was analyzed statistically with one-way ANOVA ($p < 0.05$) as this dataset consisted of two sets of points. All calculations were done with the Statistica (StatSoft) software. For some animals/hippocampus regions, the cells or dendritic fragments were not sufficiently numerous to meet the inclusion criteria for analysis. These groups are smaller than 14, which is indicated in the results section by the degrees of freedom (df) number.

Group means from the molecular analysis were analyzed for statistical significance using the *t*-test ($p < 0.05$). If not indicated differently, all data were presented as group means ± SEM.

Results

Spine density

In the CRS group, spine density in the CA1 area was significantly increased in both the apical and basal part of the pyramidal cells ($t_{24} = 5.86$, $p = 0.000005$; and $t_{26} = 3.14$, $p = 0.004$, respectively, Figure 2A) compared with controls. Likewise, a significant increase ($t_{26} = 2.63$, $p = 0.01$) in spine density was observed for the dendritic branches of the granular cells in the

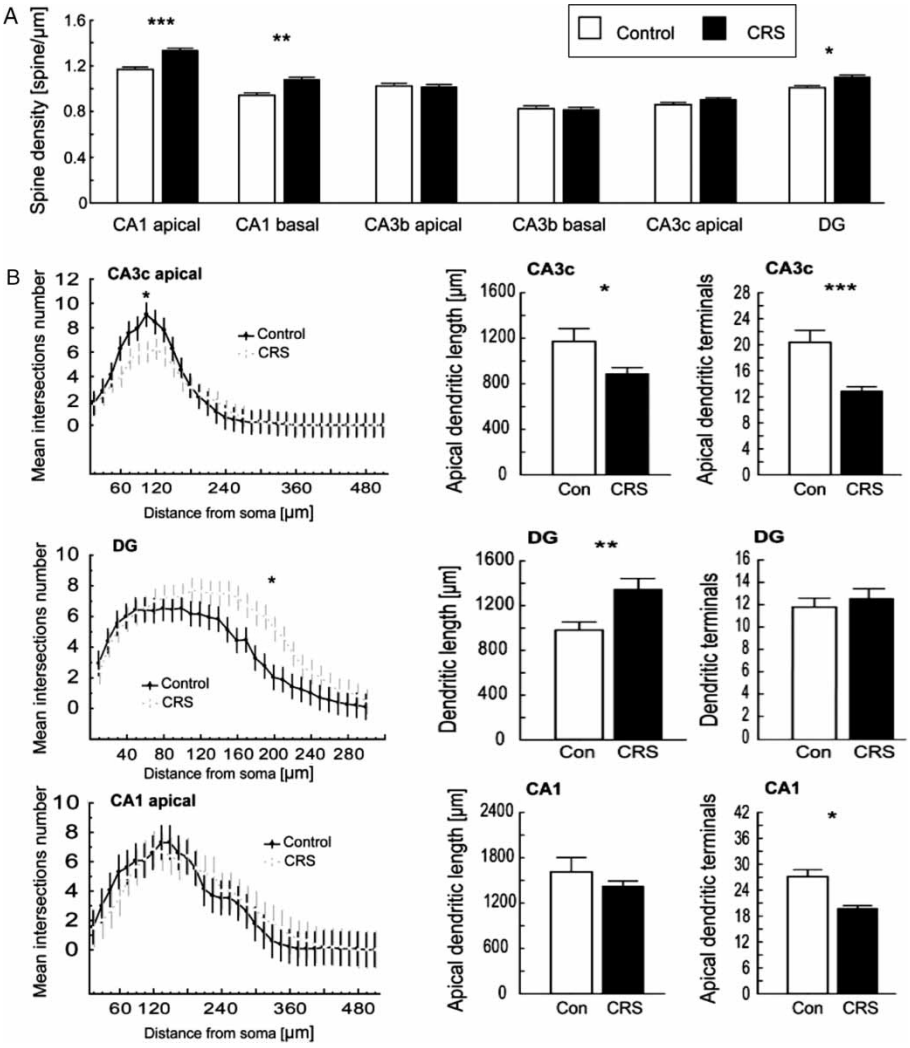

Figure 2. (A) CRS increases spine density in the CA1 and DG area with no effect in the CA3 area (mean ± SEM) $*p < 0.05$; $**p < 0.01$; $***p < 0.001$, *t*-test. (B) CRS changes the branching pattern in the apical part of the CA3c cells and in the DG granular cells, whereas the number of apical terminals in the CA1 was decreased in the CRS group $*p < 0.05$; $**p < 0.01$; $***p < 0.001$, *t*-test; bar plot shows: mean ± SEM, Sholl analysis: plots show mean values ± 95% confidence intervals (CI) (no overlapping whiskers indicate significant differences between groups with $p \leq 0.05$), one-way ANOVA.

outer half of the DG molecular layer (Figure 2A). Significant spine density changes were seen neither in the apical or basal part of the CA3b or the CA3c area (Figure 2A).

Cell morphology

In the CA1 area, morphological analysis revealed a significant ($t_{22} = 2.80$, $p = 0.02$) (Figure 2B) decrease in the total number of apical terminal branches in the CRS group, although neither the total length of the apical dendrites nor the Sholl analysis showed any significant differences. In the CA3b region, neither the number of terminal branches nor the total dendrite length differed significantly. However, in the CA3c area, CRS caused a significant decrease in the total length of dendrites ($t_{19} = 2.34$, $p = 0.03$) and number of apical terminal branches ($t_{19} = 3.99$, $p = 0.0004$) (Figure 2B). Furthermore, the Sholl analysis of the branching pattern showed a significant difference between control and CRS group (Figure 2B, $F_{1,646} = 15.57$, $p = 0.00009$). The opposite effect was observed in the DG area where an increase in the total dendritic length was observed in the CRS group (Figure 2B; $t_{24} = 3.60$, $p = 0.001$), whereas the number of DG terminal branches did not differ between the CRS group and the control group. However, the Sholl analysis showed a significant difference in the branching pattern of DG granular cells ($F_{1,719} = 139.01$, $p < 0.00001$).

Contrary to the Sholl analysis, fractal analysis did not reveal any significant changes between groups in either of the areas described above.

Real-time qPCR

To ensure that the CRS group was not statistically different from the control group with respect to the 28s/18s rRNA ratio and RNA purity, the extracted RNA was statistically evaluated. No differences were found between the control group and the CRS group in the hippocampus (data not shown). Afterwards, the mRNA levels of the eight reference genes and the seven selected postsynaptic density proteins (Spinophilin, Homer1-3, and Shank1-3) were investigated in the control group and in the CRS group with real-time qPCR. The normalized data are given in Figure 3A. The mRNA levels of Homer1 (209 ± 36%), Shank1 (138 ± 9%), Shank2 (134 ± 10%), and Spinophilin (213 ± 13%) were

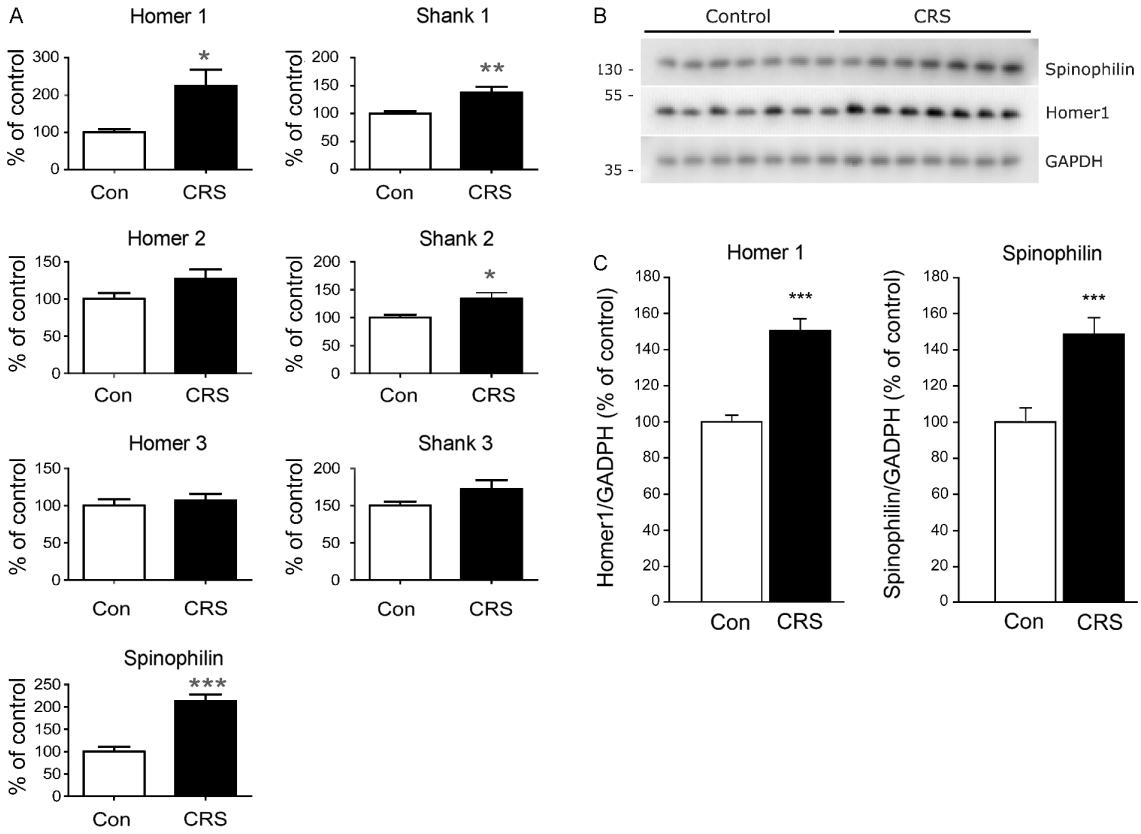

Figure 3. (A) CRS enhanced expression of genes associated with postsynaptic density. Values for each individual were normalized with the geometric mean of the reference genes, Ywhaz and Actb. Plotted data show mean group values + SEM of mRNA expression as percentage of control, * indicates significant differences between groups ($p < 0.05$, *t*-test); $n = 14$. (B) Representative immunoreactive bands from immunoblots are shown. (C) Individual bands were quantified by densitometry, normalized to GAPDH, and expressed as the mean ± SEM of control ($n = 14$ animals; ***$p < 0.001$, *t*-test). The Shank proteins could not be quantified due to low-intensity signals.

significantly upregulated in the CRS group compared with the control group. The values given in parentheses are percentage of control ± SEM.

Immunoblotting

Immunoblotting revealed stress-induced changes in protein expression levels equivalent to the changes in mRNA levels observed by real-time qPCR analysis (Figure 3B,C). Specifically, protein levels of Spinophilin (148 ± 9%) and Homer1 (151 ± 6%) were significantly upregulated in the CRS group compared with the control group. Unfortunately, we were unable to quantify the expression levels of the Shank proteins due to low-intensity signals.

Discussion

The present study supports the existing knowledge that CRS influences hippocampal spine formation and cell morphology as we find the demonstrated increase in hippocampal spine density to be paralleled by a similar increase in the expression levels of synaptic scaffolding proteins. Accordingly, CRS significantly increased the spine density in the CA1 (both apical and basal parts) and DG area. The observed increase in spine densities was followed by increased mRNA expression of the postsynaptic density proteins, Homer1, Spinophilin, and Shank1-2, and concomitant increases in the protein levels of Spinophilin and Homer1. CRS was also found to decrease the total number of terminal branches in the apical part of the CA1 and in the CA3c area, whereas the dendritic length was decreased in the CA3c area and increased in the DG area.

Our results support previous findings that restraint stress causes shortening and decreased number of apical CA3c pyramidal dendrites (Magarinos and McEwen 1995b; McLaughlin et al. 2007; Hageman et al. 2008, 2009; Vestergaard-Poulsen et al. 2011). Such changes may be elicited by an excitotoxic mechanism, because this phenomenon has been shown to depend on excitatory connections from the enthorinal cortex (Sunanda et al. 1997) and the tissue content of brain-derived neurotrophic factor (BDNF) (Magarinos et al. 2011). It may furthermore be regulated by steroid secretion via excitatory amino acids and N-Methyl-D-aspartate (NMDA) receptors (Magarinos and McEwen 1995a).

Besides Sholl analysis, we also used fractal analysis, one of the methods for quantitative assessment of ramified cell morphology (Orlowski et al. 2003). Fractal analysis has been compared with Sholl analysis, and it has sometimes been considered more sensitive (Milosevic and Ristanovic 2007) for quantification of dendritic arborization (Ristanovic et al. 2002). However, the two methods measure different aspects of cell morphology. FD describes the self-similarity of the cell shape, sometimes described as spatial complexity. This parameter alone does not completely specify the cell shape, but, in combination with other measures, such as Sholl analysis, it may give a more complete description of the cellular morphology (Smith et al. 1989). The Sholl analysis estimates the neuronal morphology more directly, describing the amount of dendrites in a certain distance from the soma, and consequently is sensitive for changes of dendrites number and length. These factors were formerly shown to be affected in CRS models of depression (Magarinos and McEwen 1995b; McLaughlin et al. 2007; Hageman et al. 2008, 2009). Our results derived from the Sholl analysis are in accordance with these findings, whereas the fractal analysis results did not reveal any differences in apical branching pattern of CA1 and CA3 cells following CRS, although it is worth mentioning that the FD measured for the whole CA1 cells was lower in the CRS group (data not shown).

Our study demonstrates that CRS increases the number of spines in CA1 and DG. However, we should state that increased spine density may not be followed by an increase in the number of functional synapses. It may be the result of a reduction in the number of functional synapses which the neurons tempt to outweigh by increasing the amount of dendritic spines (Kirov and Harris 1999).

To our knowledge, changes in DG spine density following CRS have not been reported before. The part of the DG where the number of spines was estimated receives connections from layer II of the enthorinal cortex through the perforant path, and consequently excessive input in the stress condition may lead to structural changes in the granular cell dendrites. Stress is also known to inhibit neurogenesis in DG, whereas apoptosis is enhanced (Pham et al. 2003; Czeh and Lucassen 2007). These changes might induce enhanced spine formation initially as a compensatory mechanism. In most of the previously published data on CRS models, a decrease rather than an increase of the number of spines in the CA1 has been demonstrated (McEwen 2006). Some authors have, however, reported that application of glucocorticoid receptor agonists leads to rapid spinogenesis in CA1, supporting that endogenous glucocorticoids could have a similar effect (Komatsuzaki et al. 2005). Moreover, increase in CA1 spine density has been observed in other acute (Dalla et al. 2009) or chronic stress models (Martinez-Tellez et al. 2009; McLaughlin et al. 2010; Monroy et al. 2010).

In our study, the observed spine changes were supported by increased gene and protein expression levels of postsynaptic spine proteins after CRS (Pham et al. 2003). According to Critchlow et al. (2006), expression of Spinophilin can be linked with the number of dendritic spines and therefore our comparison of the morphological and molecular data could be justified. However, we cannot definitely

conclude that the increased level of mRNA and spine proteins can be related to the observed increase in CA1 and DG spine density, as the enhanced synthesis of these proteins also could result from a higher turnover of spines, with no changes in the total number of spines. The connection between the spine density and the postsynaptic density proteins assessed in our experiment is unfortunately not straightforward because the molecular data, due to technical limitations, were analyzed in whole homogenized hippocampi. Our findings, however, can be compared with ultrastructural data obtained by Donohue et al. (2006) who found that the postsynaptic density surface area measured in the CA1 stratum lacunosum-moleculare layer was greater in animals subjected to restraint stress.

CRS may accordingly elicit a glucocorticoid-driven biphasic response where the organism and the brain initially try to adapt to the stressor by increasing the number of spines, leading to enhanced or preserved spatial memory function (Luine et al. 1996; McEwen and Gianaros 2011), whereas longer stress impact may overload the compensatory mechanisms and lead to spine loss and cognitive deficits (McEwen and Gianaros 2011; McEwen and Wingfield 2010). The CRS animals in our model could accordingly be at the stage where negative processes, like loss of CA3c dendrites, start to prevail over observed compensatory changes like CA1 and DG spine density increase.

Another explanation for the observed changes is that the animals may be habituated to the stressor, and therefore elicit an adaptive brain response, possibly resulting in increased neuroplasticity. Recently, a critical review of the stress concept and stress-related experimental paradigms has criticized the usefulness of stress models with predictable stressors, like a firmly scheduled restraint period used in our CRS model. Such experiments may stimulate the animal and lead to increased abilities, as the predictable stressor instead of being harmful may instead represent a training session for the animal (Koolhaas et al. 2011). Thus, in a study employing a CRS protocol with a very short stress duration (5 min), the authors find an enhanced spatial memory in the Morris water maze and increased hippocampal neurogenesis (Parihar et al. 2011).

Likewise, small changes in experimental procedures between CRS experiments may explain the divergent spine density results, as the animal sex, strain, age, type of stressor, type of restrainer, and time of the stress may influence the results (Magarinos and McEwen 1995a,b; McLaughlin et al. 2005, 2007, 2010; Toth et al. 2008; Dalla et al. 2009; Garrett and Wellman 2009; Parihar et al. 2011). Most of the previous studies concerning spine density and branching pattern have been done on Sprague-Dawley rats and with different stress paradigms (Magarinos and McEwen 1995b; McLaughlin et al. 2007; Hageman et al. 2008). The housing condition has also been shown to be very important as object location memory after chronic stress has been impaired in single-housed rat but not in pair-housed rats like ours (Beck and Luine 2002). Another important factor variable between CRS studies is the time of day when the stressor is applied. In the present study, the rats were stressed during the light phase, when rats are usually not very active, and had in addition a light stressor attached. Some authors have demonstrated that the stress effect may be different if the animals are restrained in the dark phase as less weight gain and increased adrenal weight could be observed here, whereas immobilization in the light phase did not cause such changes (Koolhaas et al. 2011). Therefore, CRS applied during the light period may have less effect on morphology. We should, however state that the strong light used by us during the restraint period could be an additional stress factor compared with the previous studies performed, especially when used on albino Wistar rats (Vestergaard-Poulsen et al. 2011). Another stress factor in our experimental setting could be the food restriction during the immobilization period.

In summary, we conclude that 6 h–21 days CRS causes changes in branching pattern and spine density in the Wistar rat hippocampus. The observed spine density increase was paralleled by an enhanced expression of postsynaptic density proteins involved in synaptic scaffolding. In future studies, it could be interesting to examine different stressor time lengths with the same experimental setting to further elucidate the proposed biphasic neurobiological response to CRS. However, further evaluation of this CRS protocol will also be needed to elucidate whether this paradigm, with a predictable stressor applied in the daytime, is a model mimicking chronic stress in humans.

Acknowledgments

The authors acknowledge with gratitude the skillful assistance of Ms D. Jensen, Ms T.W. Mikkelsen, and Mr A. Meier. DO was supported by Strategic Research Council, Danish Agency for Science Technology and Innovation, grant number 2106-08-0062; BE was supported by Carlsbergfondet; GW was supported by the Danish Medical Research Council (271-08-0768); and the study was supported by grants from the Lundbeck Foundation and Aarhus University.

Declaration of interest: The authors report no conflicts of interest. The authors alone are responsible for the content and writing of the paper.

References

Alquicer G, Morales-Medina JC, Quirion R, Flores G. 2008. Postweaning social isolation enhances morphological changes in

the neonatal ventral hippocampal lesion rat model of psychosis. J Chem Neuroanat 35:179–187.

Andersen CL, Jensen JL, Orntoft TF. 2004. Normalization of real-time quantitative reverse transcription-PCR data: A model-based variance estimation approach to identify genes suited for normalization, applied to bladder and colon cancer data sets. Cancer Res 64:5245–5250.

Bartesaghi R, Severi S, Guidi S. 2003. Effects of early environment on pyramidal neuron morphology in field CA1 of the guinea-pig. Neuroscience 116:715–732.

Beck KD, Luine VN. 2002. Sex differences in behavioral and neurochemical profiles after chronic stress: Role of housing conditions. Physiol Behav 75:661–673.

Bonefeld BE, Elfving B, Wegener G. 2008. Reference genes for normalization: A study of rat brain tissue. Synapse 62:302–309.

Brusco J, Wittmann R, de Azevedo MS, Lucion AB, Franci CR, Giovenardi M, Rasia-Filho AA. 2008. Plasma hormonal profiles and dendritic spine density and morphology in the hippocampal CA1 stratum radiatum, evidenced by light microscopy, of virgin and postpartum female rats. Neurosci Lett 438:346–350.

Campana AD, Sanchez F, Gamboa C, Gomez-Villalobos Mde J, De La Cruz F, Zamudio S, Flores G. 2008. Dendritic morphology on neurons from prefrontal cortex, hippocampus, and nucleus accumbens is altered in adult male mice exposed to repeated low dose of malathion. Synapse 62:283–290.

Cook SC, Wellman CL. 2004. Chronic stress alters dendritic morphology in rat medial prefrontal cortex. J Neurobiol 60: 236–248.

Critchlow HM, Maycox PR, Skepper JN, Krylova O. 2006. Clozapine and haloperidol differentially regulate dendritic spine formation and synaptogenesis in rat hippocampal neurons. Mol Cell Neurosci 32:356–365.

Czeh B, Lucassen PJ. 2007. What causes the hippocampal volume decrease in depression? Are neurogenesis, glial changes and apoptosis implicated? Eur Arch Psychiatry Clin Neurosci 257: 250–260.

Dalla C, Whetstone AS, Hodes GE, Shors TJ. 2009. Stressful experience has opposite effects on dendritic spines in the hippocampus of cycling versus masculinized females. Neurosci Lett 449:52–56.

Donohue HS, Gabbott PL, Davies HA, Rodriguez JJ, Cordero MI, Sandi C, Medvedev NI, Popov VI, Colyer FM, Peddie CJ, Stewart MG. 2006. Chronic restraint stress induces changes in synapse morphology in stratum lacunosum-moleculare CA1 rat hippocampus: A stereological and three-dimensional ultrastructural study. Neuroscience 140:597–606.

Elfving B, Bonefeld BE, Rosenberg R, Wegener G. 2008. Differential expression of synaptic vesicle proteins after repeated electroconvulsive seizures in rat frontal cortex and hippocampus. Synapse 62:662–670.

Feng J, Yan Z, Ferreira A, Tomizawa K, Liauw JA, Zhuo M, Allen PB, Ouimet CC, Greengard P. 2000. Spinophilin regulates the formation and function of dendritic spines. Proc Natl Acad Sci USA 97:9287–9292.

Garrett JE, Wellman CL. 2009. Chronic stress effects on dendritic morphology in medial prefrontal cortex: Sex differences and estrogen dependence. Neuroscience 162:195–207.

Gibb R, Kolb B. 1998. A method for vibratome sectioning of Golgi-Cox stained whole rat brain. J Neurosci Methods 79:1–4.

Gonzalez CL, Kolb B. 2003. A comparison of different models of stroke on behaviour and brain morphology. Eur J Neurosci 18: 1950–1962.

Hageman I, Nielsen M, Wortwein G, Diemer NH, Jorgensen MB. 2008. Electroconvulsive stimulations prevent stress-induced morphological changes in the hippocampus. Stress 11:282–289.

Hageman I, Nielsen M, Wortwein G, Diemer NH, Jorgensen MB. 2009. Electroconvulsive stimulations normalizes stress-induced changes in the glucocorticoid receptor and behaviour. Behav Brain Res 196:71–77.

Kirov SA, Harris KM. 1999. Dendrites are more spiny on mature hippocampal neurons when synapses are inactivated. Nat Neurosci 2:878–883.

Komatsuzaki Y, Murakami G, Tsurugizawa T, Mukai H, Tanabe N, Mitsuhashi K, Kawata M, Kimoto T, Ooishi Y, Kawato S. 2005. Rapid spinogenesis of pyramidal neurons induced by activation of glucocorticoid receptors in adult male rat hippocampus. Biochem Biophys Res Commun 335:1002–1007.

Koolhaas JM, Bartolomucci A, Buwalda B, de Boer SF, Flügge G, Korte SM, Meerlo P, Murison R, Olivier B, Palanza P, Richter-Levin G, Sgoifo A, Steimer T, Stiedl O, van Dijk G, Wöhr M, Fuchs E. 2011. Stress revisited: A critical evaluation of the stress concept. Neurosci Biobehav Rev 35:1291–1301.

Luine V, Martinez C, Villegas M, Magarinos AM, McEwen BS. 1996. Restraint stress reversibly enhances spatial memory performance. Physiol Behav 59:27–32.

Magarinos AM, McEwen BS. 1995a. Stress-induced atrophy of apical dendrites of hippocampal CA3c neurons: Involvement of glucocorticoid secretion and excitatory amino acid receptors. Neuroscience 69:89–98.

Magarinos AM, McEwen BS. 1995b. Stress-induced atrophy of apical dendrites of hippocampal CA3c neurons: Comparison of stressors. Neuroscience 69:83–88.

Magarinos AM, Li CJ, Toth JG, Bath KG, Jing D, Lee FS, McEwen BS. 2011. Effect of brain-derived neurotrophic factor haploinsufficiency on stress-induced remodeling of hippocampal neurons. Hippocampus 21:253–264.

Martinez-Tellez RI, Hernandez-Torres E, Gamboa C, Flores G. 2009. Prenatal stress alters spine density and dendritic length of nucleus accumbens and hippocampus neurons in rat offspring. Synapse 63:794–804.

McEwen BS. 1999. Stress and hippocampal plasticity. Annu Rev Neurosci 22:105–122.

McEwen BS. 2006. Protective and damaging effects of stress mediators: Central role of the brain. Dialogues Clin Neurosci 8: 367–381.

McEwen BS. 2008. Central effects of stress hormones in health and disease: Understanding the protective and damaging effects of stress and stress mediators. Eur J Pharmacol 583:174–185.

McEwen BS, Gianaros PJ. 2011. Stress- and allostasis-induced brain plasticity. Annu Rev Med 62:431–445.

McEwen BS, Wingfield JC. 2010. What is in a name? Integrating homeostasis, allostasis and stress. Horm Behav 57:105–111.

McLaughlin KJ, Baran SE, Wright RL, Conrad CD. 2005. Chronic stress enhances spatial memory in ovariectomized female rats despite CA3 dendritic retraction: Possible involvement of CA1 neurons. Neuroscience 135:1045–1054.

McLaughlin KJ, Gomez JL, Baran SE, Conrad CD. 2007. The effects of chronic stress on hippocampal morphology and function: An evaluation of chronic restraint paradigms. Brain Res 1161:56–64.

McLaughlin KJ, Wilson JO, Harman J, Wright RL, Wieczorek L, Gomez J, Korol DL, Conrad CD. 2010. Chronic 17beta-estradiol or cholesterol prevents stress-induced hippocampal CA3 dendritic retraction in ovariectomized female rats: Possible correspondence between CA1 spine properties and spatial acquisition. Hippocampus 20:768–786.

Milosevic NT, Ristanovic D. 2007. The Sholl analysis of neuronal cell images: Semi-log or log-log method? J Theor Biol 245: 130–140.

Monroy E, Hernandez-Torres E, Flores G. 2010. Maternal separation disrupts dendritic morphology of neurons in prefrontal cortex, hippocampus, and nucleus accumbens in male rat offspring. J Chem Neuroanat 40:93–101.

Orlowski D, Bjarkam CR. 2009. Autometallographic enhancement of the Golgi-Cox staining enables high resolution visualization of dendrites and spines. Histochem Cell Biol 132:369–374.

Orlowski D, Soltys Z, Janeczko K. 2003. Morphological development of microglia in the postnatal rat brain. A quantitative study. Int J Dev Neurosci 21:445–450.

Parihar VK, Hattiangady B, Kuruba R, Shuai B, Shetty AK. 2011. Predictable chronic mild stress improves mood, hippocampal neurogenesis and memory. Mol Psychiatry 16:171–183.

Pham K, Nacher J, Hof PR, McEwen BS. 2003. Repeated restraint stress suppresses neurogenesis and induces biphasic PSA-NCAM expression in the adult rat dentate gyrus. Eur J Neurosci 17:879–886.

Ristanovic D, Nedeljkov V, Stefanovic BD, Milosevic NT, Grgurevic M, Stulic V. 2002. Fractal and nonfractal analysis of cell images: Comparison and application to neuronal dendritic arborization. Biol Cybern 87:278–288.

Sala C, Piech V, Wilson NR, Passafaro M, Liu G, Sheng M. 2001. Regulation of dendritic spine morphology and synaptic function by Shank and Homer. Neuron 31:115–130.

Sarrouilhe D, di Tommaso A, Metaye T, Ladeveze V. 2006. Spinophilin: From partners to functions. Biochimie 88: 1099–1113.

Shi SH, Cox DN, Wang D, Jan LY, Jan YN. 2004. Control of dendrite arborization by an Ig family member, dendrite arborization and synapse maturation 1 (Dasm1). Proc Natl Acad Sci USA 101:13341–13345.

Sholl DA. 1953. Dendritic organization in the neurons of the visual and motor cortices of the cat. J Anat 87:387–406.

Shors TJ, Falduto J, Leuner B. 2004. The opposite effects of stress on dendritic spines in male vs. female rats are NMDA receptor-dependent. Eur J Neurosci 19:145–150.

Smith TG, Jr, Marks WB, Lange GD, Sheriff WH, Jr, Neale EA. 1989. A fractal analysis of cell images. J Neurosci Methods 27:173–180.

Sunanda, Meti BL, Raju TR. 1997. Entorhinal cortex lesioning protects hippocampal CA3 neurons from stress-induced damage. Brain Res 770:302–306.

Tata DA, Anderson BJ. 2010. The effects of chronic glucocorticoid exposure on dendritic length, synapse numbers and glial volume in animal models: Implications for hippocampal volume reductions in depression. Physiol Behav 99:186–193.

Toth E, Gersner R, Wilf-Yarkoni A, Raizel H, Dar D, Richter-Levin G, Levit O, Zangen A. 2008. Age-dependent effects of chronic stress on brain plasticity and depressive behavior. J Neurochem 107:522–532.

Vestergaard-Poulsen P, Wegener G, Hansen B, Bjarkam CR, Blackband SJ, Nielsen NC, Jespersen SN. 2011. Diffusion-weighted MRI and quantitative biophysical modeling of hippocampal neurite loss in chronic stress. PLoS ONE 6:e20653.

Watanabe Y, Gould E, McEwen BS. 1992. Stress induces atrophy of apical dendrites of hippocampal CA3 pyramidal neurons. Brain Res 588:341–345.

Woolley CS, Gould E, McEwen BS. 1990. Exposure to excess glucocorticoids alters dendritic morphology of adult hippocampal pyramidal neurons. Brain Res 531:225–231.